# Pattern Formation by Graded and Uniform Signals in the Early *Drosophila* Embryo

Jitendra S. Kanodia,[†‡△] Hsiao-Lan Liang,[§∥△] Yoosik Kim,[†‡] Bomyi Lim,[†‡] Mei Zhan,[¶] Hang Lu,[¶] Christine A. Rushlow,[§*] and Stanislav Y. Shvartsman[†‡*]

[†]Department of Chemical and Biological Engineering and [‡]Lewis-Sigler Institute for Integrative Genomics, Princeton University, Princeton, New Jersey; [§]Center for Developmental Genetics, Department of Biology, New York University, New York, New York; and [¶]School of Chemical and Biomolecular Engineering and [∥]Parker H. Petit Institute for Bioengineering and Bioscience, Georgia Institute of Technology, Atlanta, Georgia

ABSTRACT   The early *Drosophila* embryo is patterned by graded distributions of maternal transcription factors. Recent studies revealed that pattern formation by these graded signals depends on uniformly expressed transcriptional activators, such as Zelda. Removal of Zelda influences both the timing and the spatial expression domains for most of the genes controlled by maternal gradients. We demonstrate that some of these patterning defects, which range from temporal delay to loss of expression, can be rationalized with the use of a mathematical model based on cooperative binding of graded and uniform factors. This model makes a number of predictions, which we confirm experimentally by analyzing the expression of *short gastrulation* (*sog*), a gene that is controlled by a combination of the Dorsal morphogen gradient and Zelda. The proposed model suggests a general mechanism for the formation of nested gene expression domains, which is a hallmark of tissue patterning by morphogen gradients. According to this mechanism, the differential effects of a morphogen on its target genes can depend on their differential sensitivity to uniform factors.

## INTRODUCTION

Early stages of *Drosophila* development rely on graded distributions of transcription factors in the precellular embryo. The anterior-to-posterior gradient of Bicoid (Bcd), a transcriptional activator, specifies the anterior body segments (1). The ventral-to-dorsal nuclear localization gradient of Dorsal (Dl), which can both activate and repress gene expression, organizes the spatial arrangement of the mesoderm, neural ectoderm, and dorsal ectoderm tissues (2). Graded distribution of a transcriptional repressor Capicua (Cic), with minima at both anterior and posterior poles, patterns the nonsegmented terminal regions of the embryo (3,4). Established by three independent maternal systems, the Bcd, Dl, and Cic gradients provide inputs to the *cis*-regulatory modules of genes involved in multiple aspects of early embryogenesis.

Gene regulation by Bcd, Dl, and Cic depends on interactions between the morphogens themselves and between morphogens and their transcriptional targets. For instance, the anterior expression of *tailless* (*tll*) depends on its direct activation by Bcd and derepression by Cic (5). Combinatorial effects of this type are also present in transcriptional cascades, when a gene is regulated by a morphogen both directly and through a more proximal target (6). For example, genes involved in patterning the presumptive ectoderm region, such as *short gastrulation* (*sog*), are controlled by the Dl gradient both directly and through *snail* (*sna*), which is induced by Dl.

Recent studies revealed that the effects of maternal morphogens are dramatically affected by uniformly expressed transcriptional activators, such as Zelda (Zld) (7) and Stat92E (8). In particular, removal of Zld affects most of the canonical targets of the Bcd, Dl, and Cic gradients (9). Patterning defects induced by loss of Zld range from delayed expression and alteration of gene expression domains to significant loss of expression. The main purpose of this work is to present a model that can be used as a first step in the quantitative analysis of these effects.

## MATERIALS AND METHODS

### Fly strains

OreR flies were used as the wild-type (WT) strain for all experiments, and *zld*[−] embryos were obtained from germ-line clones derived from females of genotype *zld*[294] *FRT19A/ovo*[D] as previously described (8).

### Immunostaining and fluorescence in situ hybridization

Mouse anti-Dl (1:100 monoclonal antibody from Developmental Studies Hybridoma Bank), and rat anti-Zld (1:200) (7,9) were used as the primary antibodies. DAPI (4′,6-diamidino-2-phenylindole, 1:10,000; Vector Laboratories) was used to stain the nuclei, and Alexa Fluor conjugates (1:500; Invitrogen) were used as secondary antibodies. To visualize the *sog* transcript, fluorescence in situ hybridization (FISH) was used as described previously (10). Embryos were hybridized with digoxigenin (DIG)-labeled antisense probe to *sog* introns overnight at 60°C. Sheep anti-DIG (1:125; Roche) was used as the primary antibody, and Alexa Fluors (1:500) were used as secondary antibodies.

## Microscopy and quantification

Imaging was performed with a Zeiss LSM 510 confocal microscope with a Zeiss 40×numerical aperture 1.2 C-Apo water-immersion objective. High-resolution images (512 × 512 pixels, 12 bit depth) were obtained. All images were collected at the focal plane ~70 $\mu$m from either the anterior or posterior pole. Embryos were imaged in 90% glycerol solution. The mean profile and the corresponding 99% confidence intervals for *sog* expression were estimated as described previously (10). The statistical significance of a decrease in Zld with time was obtained by linear regression of the Zld level with the mid-point of time for the corresponding nuclear cycle.

## RESULTS AND DISCUSSION

### Equilibrium binding model

Zld binds to the *cis*-regulatory modules of essentially all known transcriptional targets of maternal morphogens (9). Furthermore, Zld-binding sites are often found close to the binding sites of spatially distributed regulators, such as Bcd and Dl. On the basis of these observations, we hypothesize that the patterning effects of Zld can be explained by cooperative interactions between Zld and a morphogen, such as Bcd or Dl. To illustrate this point, we analyze the activity of a hypothetical regulatory region of a gene controlled by two transcription factors, *A* and *B*. The concentrations of these factors are denoted by $C_A$ and $C_B$. Let us think of $C_A$ as the concentration of a morphogen, such as Dl, and $C_B$ as the concentration of a uniform activator, such as Zld. The regulatory region can be found in four different states: one state with both sites empty, two states with a single site occupied, and one state with both sites bound by their corresponding transcription factors (Fig. 1 *A*).

For most of the genes, removal of Zld delays or diminishes expression, whereas removal of graded activators, such as Bcd and Dl, leads to a complete loss of expression (7,9). Based on this, we assume that binding of a morphogen is necessary for transcriptional activation, and that the uniform factor increases the morphogen binding or activity. Thus, within the framework of our model, transcription is supported by two states: one in which *A* is bound on its own, and one in which it is bound together with *B* (Fig. 1 *A*).

When the binding reactions are in equilibrium, the probability of finding the regulatory region in either one of these states is given by the following formula (11,12):

$$P\{A \text{ bound}\} = P\{A\} + P\{A\&B\}$$
$$= \frac{C_A + C_A C_B \omega / K_B}{K_A + C_A + K_A C_B / K_B + C_A C_B \omega / K_B}.$$
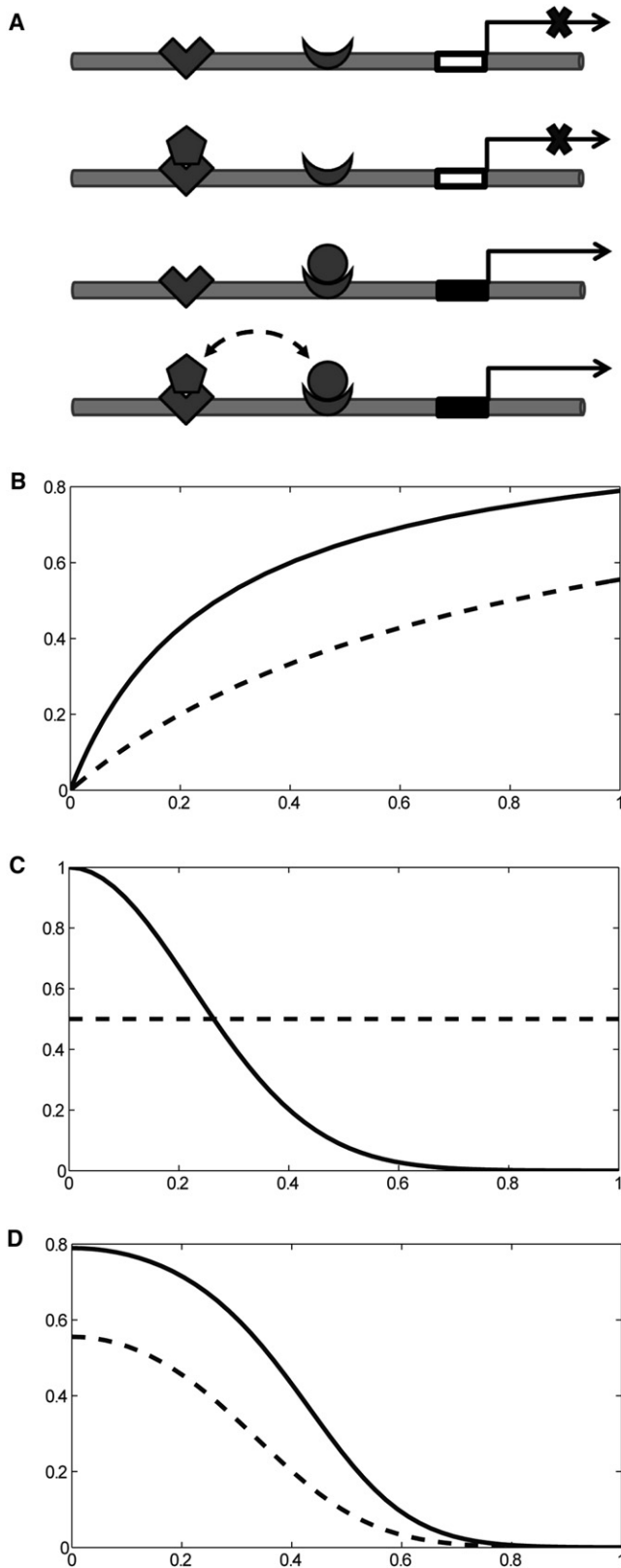
FIGURE 1 Site occupancy model for gene regulation by the graded factor, *A* (*circle*), and the uniform factor, *B* (*pentagon*). (*B*) Activity of the regulatory region as a function of the level of the graded factor in the presence and absence of the uniform factor (*solid and dashed lines*, respec-tively). (*C*) Spatial distributions of the concentrations of graded and uniform factors, $C_A$ and $C_B$, respectively; $x$ denotes the distance from the point that corresponds to the maximum of $C_A$. (*D*) Spatial pattern of the activity of the regulatory region in the presence and absence of the uniform factor (*solid and dashed lines*, respectively).

$K_A$ and $K_B$ are the corresponding equilibrium binding constants, which characterize the binding affinities of $A$ and $B$ to their respective sites, when taken in isolation. $\omega$ is a measure of cooperativity, which reflects the ability of factor $B$ to change the binding affinity of $A$ to its site. Note that expression for $P\{A \text{ bound}\}$ can be written as:

$$P\{A \text{ bound}\} = \frac{C_A}{K_A f(\omega, C_B, K_B) + C_A},$$

where

$$f(\omega, C_B, K_B) = \frac{1 + C_B/K_B}{1 + \omega C_B/K_B}.$$

Thus, the effect of a uniform factor amounts to changing the equilibrium binding constant of the graded factor. Clearly, when $\omega = 1$, $f(\omega, C_B, K_B) = 1$, and the probability of expression reduces to $P\{A\} = C_A/(C_A + K_A)$. This corresponds to the case of no cooperativity. On the other hand, when $\omega > 1$, $f(\omega, C_B, K_B) < 1$ and the equilibrium binding constant is lower than $K_A$. In this case, factor $B$ can be viewed as a coactivator that facilitates binding of factor $A$. In this case, the output of the regulatory region at any given level of $C_A$ is reduced by removal of the uniform factor ($C_B = 0$) or its binding site ($K_B = \infty$). Either one of these perturbations reduces $P\{A \text{ bound}\}$ throughout the patterned tissue (Fig. 1, B–D).

## Experimental tests of the model

As a first step toward testing this model, we analyzed the expression of *sog*, a gene that is controlled by both Zld, which is uniform, and nuclear Dl, which is graded (Fig. 2 A). The graded distribution of nuclear Dl establishes the expression patterns of multiple genes involved in subdividing the embryo into three germ layers: mesoderm, neural ectoderm, and dorsal ectoderm (Fig. 2 B) (2,6). The future mesoderm is marked by ventrally expressed genes, such as *sna*. The future neuroectoderm is specified by genes expressed in two symmetric lateral stripes, such as the pattern of *sog*. Finally, the dorsal ectoderm is defined by dorsally expressed genes, such as *decapentaplegic* (*dpp*). Of importance, most of the genes expressed in these three domains are affected by removal of Zld and have Zld-binding sites in their regulatory regions (9,13).

The lateral expression stripes of *sog* are controlled by two enhancers, both of which contain multiple interspersed binding sites for Dl and Zld (Fig. 2 C). This is a common feature of many genes that are controlled by the graded distribution of nuclear Dl (9,13–15). The ventral border of the *sog* pattern is sharp and determined by the repressive effect of Sna (2), which is itself a target of Dl and Zld. The dorsal border, on the other hand, is graded and is believed to reflect limiting levels of Dl. In testing our model, we focused on the dorsal part of the *sog* pattern.

In the absence of Zld, the broad lateral pattern of *sog* is reduced to a much narrower domain, within which <40% of cells exhibit detectable transcripts (8). Previous studies of this effect were based on lateral views of the *sog* expression domain in a handful of embryos (7,9). To explore the effect of Zld quantitatively and throughout the DV axis, we analyzed *sog* expression in a large number of embryos, using a microfluidic device that enables large-scale imaging of embryos in cross-sectional views (16).

We used in situ hybridization assays with probes directed against intronic *sog* sequences (Fig. 2, D and E). Intronic transcripts are more unstable than the corresponding cytoplasmic mRNA. As a consequence, in situ hybridization with intronic probes provides information about transcription in a much shorter time interval than that assessed by hybridization with probes against the coding region (10). Thus, the expression of introns is a proxy for the rate of transcription and can be used to test our model of gene regulation by graded and uniform signals.

We quantified the *sog* pattern in WT and *zld*⁻ backgrounds using our previously developed image processing algorithm, which identifies intronic staining in the nuclei of embryos costained with the *sog* probe and Dl antibodies (10). The maximum of the nuclear Dl gradient defines the ventralmost position along the DV axis. The main output of image processing is a vector with binary components (1/0), which correspond to the presence (1) or absence (0) of *sog* intronic signal at different positions along the DV axis (Fig. 2, D and E, right panels). By combining such vectors from multiple embryos, we estimated the probability of *sog* expression along the DV axis (Fig. 2, F and G).

Consistent with the model, we found that the probability of *sog* expression in the *zld*⁻ background is significantly lower than the probability of *sog* expression in WT embryos throughout the entire neuroectoderm region. A lower probability of *sog* expression implies that the pattern of *sog* would be more narrow and patchy than that in WT, which is consistent with and explains previous observations (9). An additional test of our model is provided by an analysis of *sog* expression at different time points. Levels of nuclear Dl increase during the last five nuclear division cycles in the syncytial blastoderm (17,18). In our model, removal of Zld leaves Dl as the only regulator of *sog* in the presumptive neuroectoderm region. If the increase in the levels of nuclear Dl is functionally significant, it should lead to an increase of the probability of *sog* expression in the absence of Zld. By comparing the spatial patterns of the probability of *sog* expression in *zld*⁻ in two consecutive nuclear cycles, we found that this is indeed the case (Fig. 3 A).

On the other hand, there was essentially no change in *sog* expression in the WT background (Fig. 3 B). Within the framework of our model, this stability can be explained only if an increase in the level of nuclear Dl is accompanied
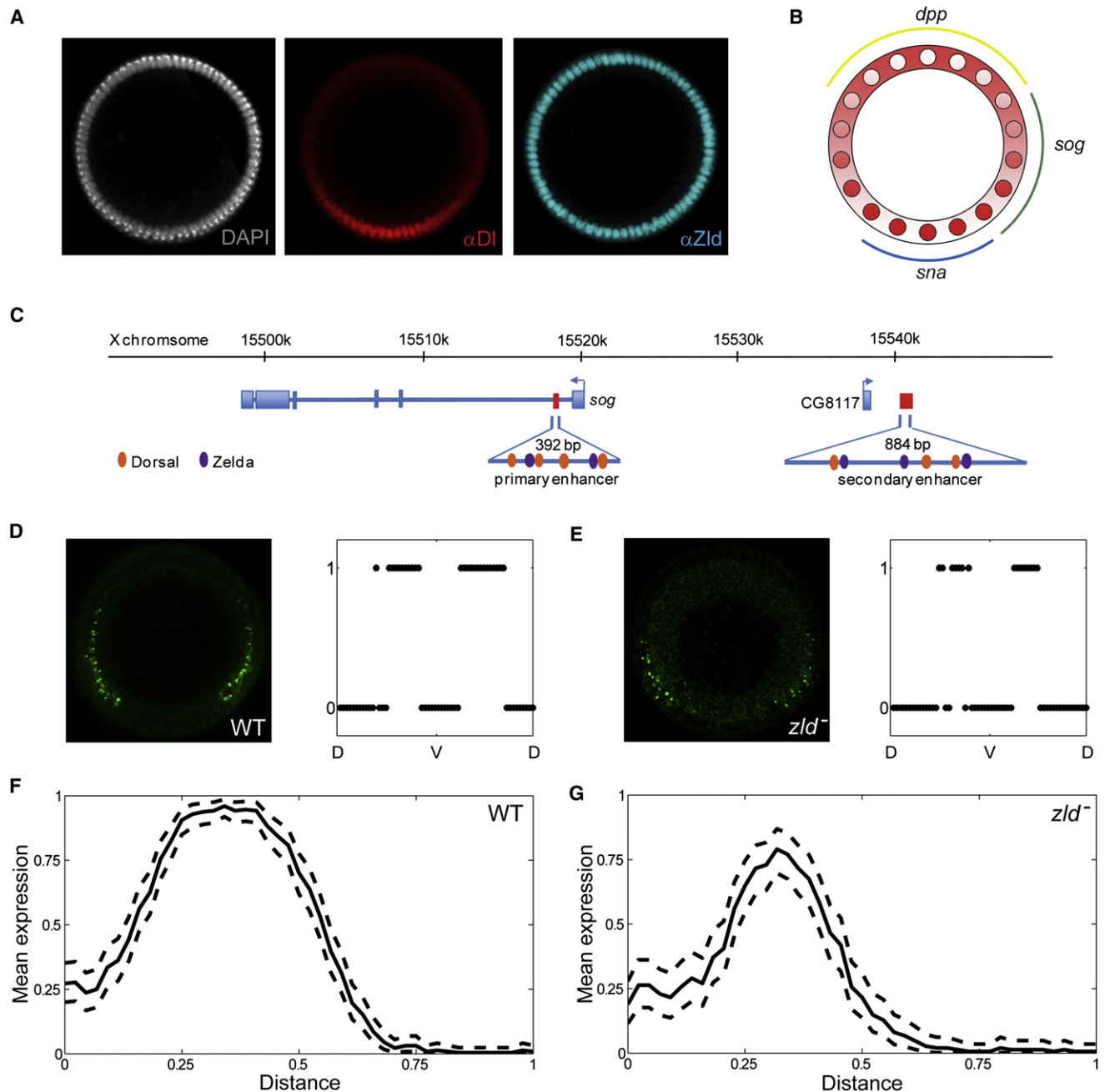
FIGURE 2 Regulation of *sog* by Dl and Zld. (*A*) DV patterning system, showing a spatially uniform arrangement of nuclei (*white*), graded distribution of nuclear Dl (*red*), and spatially uniform distribution of Zld (*cyan*) in the syncytial blastoderm stage of *Drosophila* embryogenesis. (*B*) The Dl gradient subdivides the embryo into three domains that give rise to the future muscle, nerve, and skin tissues. These domains are marked by the expression of *sna* (*blue*), *sog* (*green*), and *dpp* (*yellow*). (*C*) Schematic representation of the *sog* region. Exons (*blue rectangles*), introns (*blue lines*), and enhancers (*red rectangles*) are shown. Cognate binding sites for Dl and Zld are depicted as ovals in orange and purple, respectively. Note that the secondary shadow enhancer lies downstream of the neighboring gene, CG8117 (35). (*D*) *sog* intronic expression in cross-sectional view (*left*) and the corresponding expression profile along the DV axis (*right*) for a representative WT embryo during nuclear cycle 14. (*E*) *sog* intronic expression in cross-sectional view (*left*) and the corresponding expression profile along DV axis (*right*) for a representative *zld⁻* embryo during nuclear cycle 14. (*F*) WT expression profile of *sog* in nuclear cycle 14. The solid curve represents the mean profile; dashed curves show the 99% confidence intervals of the mean. Along the horizontal axis, *x* denotes the normalized distance along the DV axis, and 0/1 correspond to the ventralmost/dorsalmost positions, respectively. (*G*) *sog* expression in *zld⁻* embryos during nuclear cycle 14. Throughout the neuroectoderm region, the *sog* expression level is significantly lower than that in WT.

by a decrease in the level of Zld. In agreement with this scenario, we found that the levels of Zld show a statistically significant decrease over several consecutive nuclear divi-

sion cycles (Fig. 3 *C*). Based on this, we conclude that *sog* expression reflects a combination of increasing levels of Dl and decreasing level of Zld. Finally, we note that
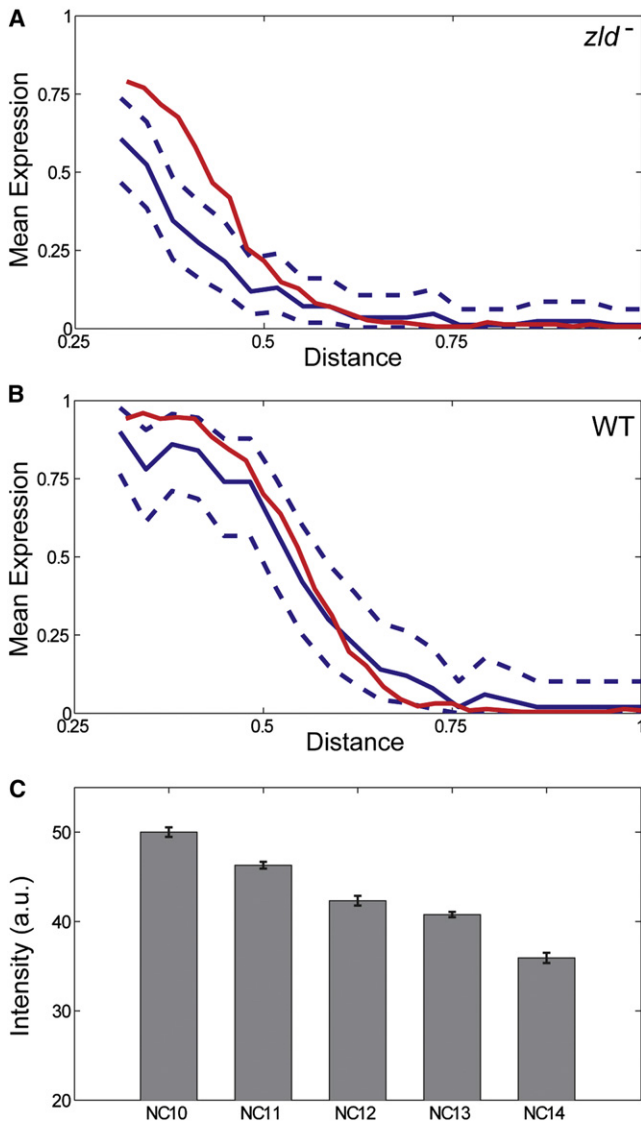
FIGURE 3 Dynamics of *sog* expression. (*A*) Quantitative comparison of the mean intensities of the *sog* FISH signal in *zld⁻* embryos during nuclear cycles 13 (*solid blue*) to the mean signal in cycle 14 (*solid red*). Dashed blue curves correspond to the 99% confidence interval for mean expression level in cycle 13. For clarity, *sog* expression in the presumptive mesoderm ($0 < x < 0.25$) has been omitted. (*B*) Quantitative comparison of the mean intensities of the *sog* FISH signal in the nuclear cycles 13 (*solid blue*) and 14 (*solid red*) of WT embryos. Dashed curves correspond to the 99% confidence interval for mean *sog* expression profile in nuclear cycle 13. The mean values are not significantly different throughout the neuroectoderm region. (*C*) Dynamics of the nuclear levels of Zld over five nuclear cycles. The levels of Zld decrease as a function of developmental time ($p < 0.001$).

*sog* introns are first detectable during nuclear cycle 11 in WT embryos (9). On the other hand, they do not appear until nuclear cycle 13 in *zld⁻* embryos (9). This delay can be explained by the fact that the low level of Dl at nuclear cycle 11 requires Zld to activate *sog* gene transcription. In the absence of Zld, the lower level of Dl at nuclear cycle 11 is not sufficient, and *sog* is activated only at later times when the levels of Dl are higher.

## CONCLUSION

The presented model provides a straightforward explanation for the effects of Zld on the spatiotemporal pattern of *sog* expression. Admittedly, this model is a simplification of *sog* regulation, which depends on two different enhancers, each of which has multiple Dl- and Zld-binding sites. At the same time, this model explains the decrease in the rate of *sog* transcription, the time delay in the initiation of *sog* expression, and the sporadic nature of *sog* expression in the absence of Zld. How Zld influences binding of Dl and other morphogens to their cognate DNA sequences is currently unknown. Cooperative effects in transcription are not restricted to direct protein-protein contacts, as in the canonical regulated recruitment models (19), and may be more complex (e.g., they can be mediated by displacement of nucleosomes (20)).

A similar model can be used to explore the effects of Zld on pattern formation by other graded signals, such as Bcd, which patterns the AP axis of the embryo. Furthermore, Zld can affect pattern formation by secondary graded signals that are induced by maternal gradients. For example, a graded pattern of Dpp signaling is established by an elaborate transcriptional and signaling cascade downstream of the Dl gradient (21–25). Of interest, a number of Dpp target genes have Zld-binding sites in their regulatory regions, and the expression domains of these genes potentially can be interpreted with the use of a model similar to the one presented in this study (9). Likewise, a number of transcriptional targets of *sna*, which is itself induced by Dl, have Zld-binding sites (9). Thus, our model can be used to understand both direct and indirect effects of maternal morphogen gradients.

The proposed model provides a mechanism for the formation of nested gene expression domains, which is a hallmark of tissue patterning by morphogen gradients (26). This feature has been attributed to a differential enhancer response to a graded factor (27–33), or to the combinatorial effects of graded signals (5,34). In our model, enhancers with the exact same binding strengths for the graded factor but different binding sites for the uniform factor can be differentially activated by a morphogen (Fig. 4). According to this model, removal of a uniform factor can make a number of different gene expression borders collapse to the same location, an effect that indeed has been observed in response to removal of Zld (9). On the basis of these findings, we propose that differential sensitivity to uniformly expressed factors can contribute to the formation of nested gene expression domains in the *Drosophila* embryo and other systems patterned by morphogens.
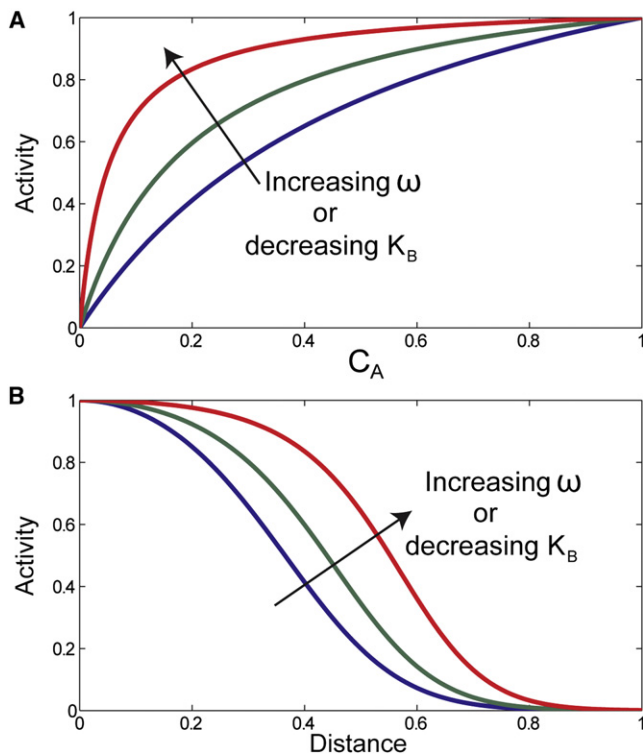
FIGURE 4   Proposed model for the formation of nested gene expression patterns. (*A*) The activity of a gene regulatory region controlled by graded and uniform factors (*A* and *B*, respectively) can be affected by the binding strength of the uniform factor ($K_B$) and/or the cooperativity parameters ($\omega$). The three curves can be viewed as response functions of three hypothetical target genes. All three curves were calculated for the same value of $K_A$, the binding strength of the uniform factor. (*B*) Changes in the values of $K_B$ and $\omega$ give rise to the corresponding changes of expression domains. In the absence of a uniform factor, all three genes will be expressed in the same domain. All three curves were calculated for the same value of $K_A$.

## REFERENCES

1. Porcher, A., and N. Dostatni. 2010. The bicoid morphogen system. *Curr. Biol.* 20:R249–R254.

2. Hong, J. W., D. A. Hendrix, …, M. S. Levine. 2008. How the Dorsal gradient works: insights from postgenome technologies. *Proc. Natl. Acad. Sci. USA.* 105:20072–20076.

3. Ajuria, L., C. Nieva, …, G. Jiménez. 2011. Capicua DNA-binding sites are general response elements for RTK signaling in Drosophila. *Development.* 138:915–924.

4. Jiménez, G., A. Guichet, …, J. Casanova. 2000. Relief of gene repression by torso RTK signaling: role of *capicua* in *Drosophila* terminal and dorsoventral patterning. *Genes Dev.* 14:224–231.

5. Löhr, U., H.-R. Chung, …, H. Jäckle. 2009. Antagonistic action of Bicoid and the repressor Capicua determines the spatial limits of *Drosophila* head gene expression domains. *Proc. Natl. Acad. Sci. USA.* 106:21695–21700.

6. Chopra, V. S., and M. Levine. 2009. Combinatorial patterning mechanisms in the *Drosophila* embryo. *Brief. Funct. Genomics Proteomics.* 8:243–249.

7. Liang, H. L., C. Y. Nien, …, C. Rushlow. 2008. The zinc-finger protein Zelda is a key activator of the early zygotic genome in *Drosophila*. *Nature.* 456:400–403.

8. Tsurumi, A., F. Xia, …, W. X. Li. 2011. STAT is an essential activator of the zygotic genome in the early *Drosophila* embryo. *PLoS Genet.* 7:e1002086.

9. Nien, C. Y., H. L. Liang, …, C. Rushlow. 2011. Temporal coordination of gene networks by Zelda in the early *Drosophila* embryo. *PLoS Genet.* 7:e1002339.

10. Kanodia, J. S., Y. Kim, …, S. Y. Shvartsman. 2011. A computational statistics approach for estimating the spatial range of morphogen gradients. *Development.* 138:4867–4874.

11. Bintu, L., N. E. Buchler, …, R. Phillips. 2005. Transcriptional regulation by the numbers: applications. *Curr. Opin. Genet. Dev.* 15:125–135.

12. Bintu, L., N. E. Buchler, …, R. Phillips. 2005. Transcriptional regulation by the numbers: models. *Curr. Opin. Genet. Dev.* 15:116–124.

13. Harrison, M. M., X. Y. Li, …, M. B. Eisen. 2011. Zelda binding in the early *Drosophila melanogaster* embryo marks regions subsequently activated at the maternal-to-zygotic transition. *PLoS Genet.* 7:e1002266.

14. Markstein, M., R. Zinzen, …, M. Levine. 2004. A regulatory code for neurogenic gene expression in the *Drosophila* embryo. *Development.* 131:2387–2394.

15. Liberman, L. M., and A. Stathopoulos. 2009. Design flexibility in *cis*-regulatory control of gene expression: synthetic and comparative evidence. *Dev. Biol.* 327:578–589.

16. Chung, K., Y. Kim, …, H. Lu. 2011. A microfluidic array for large-scale ordering and orientation of embryos. *Nat. Methods.* 8:171–176.

17. Kanodia, J. S., R. Rikhy, …, S. Y. Shvartsman. 2009. Dynamics of the Dorsal morphogen gradient. *Proc. Natl. Acad. Sci. USA.* 106:21707–21712.

18. Liberman, L. M., G. T. Reeves, and A. Stathopoulos. 2009. Quantitative imaging of the Dorsal nuclear gradient reveals limitations to threshold-dependent patterning in *Drosophila*. *Proc. Natl. Acad. Sci. USA.* 106:22317–22322.

19. Ptashne, M., and A. Gann. 2001. Genes & Signals. Spring Harbor Laboratory Press, Cold Spring Harbor, NY.

20. Mirny, L. A. 2010. Nucleosome-mediated cooperativity between transcription factors. *Proc. Natl. Acad. Sci. USA.* 107:22534–22539.

21. Lin, M. C., J. Park, …, C. Rushlow. 2006. Threshold response of C15 to the Dpp gradient in *Drosophila* is established by the cumulative effect of Smad and Zen activators and negative cues. *Development.* 133:4805–4813.

22. Xu, M., N. Kirov, and C. Rushlow. 2005. Peak levels of BMP in the *Drosophila* embryo control target genes by a feed-forward mechanism. *Development.* 132:1637–1647.

23. Mizutani, C. M., N. Meyer, …, E. Bier. 2006. Threshold-dependent BMP-mediated repression: a model for a conserved mechanism that patterns the neuroectoderm. *PLoS Biol.* 4:e313.

24. Mizutani, C. M., Q. Nie, …, A. D. Lander. 2005. Formation of the BMP activity gradient in the *Drosophila* embryo. *Dev. Cell.* 8:915–924.

25. O'Connor, M. B., D. Umulis, …, S. S. Blair. 2006. Shaping BMP morphogen gradients in the *Drosophila* embryo and pupal wing. *Development.* 133:183–193.

26. Ashe, H. L., and J. Briscoe. 2006. The interpretation of morphogen gradients. *Development.* 133:385–394.

27. Struhl, G., K. Struhl, and P. M. Macdonald. 1989. The gradient morphogen bicoid is a concentration-dependent transcriptional activator. *Cell.* 57:1259–1273.

28. Driever, W., and C. Nüsslein-Volhard. 1988. The bicoid protein determines position in the *Drosophila* embryo in a concentration-dependent manner. *Cell.* 54:95–104.

29. Driever, W., G. Thoma, and C. Nüsslein-Volhard. 1989. Determination of spatial domains of zygotic gene expression in the *Drosophila* embryo by the affinity of binding sites for the *bicoid* morphogen. *Nature.* 340:363–367.

30. Jiang, J., D. Kosman, …, M. Levine. 1991. The dorsal morphogen gradient regulates the mesoderm determinant *twist* in early *Drosophila* embryos. *Genes Dev.* 5:1881–1891.

31. Jiang, J., and M. Levine. 1993. Binding affinities and cooperative interactions with bHLH activators delimit threshold responses to the dorsal gradient morphogen. *Cell.* 72:741–752.

32. Papatsenko, D., and M. Levine. 2005. Quantitative analysis of binding motifs mediating diverse spatial readouts of the Dorsal gradient in the *Drosophila* embryo. *Proc. Natl. Acad. Sci. USA.* 102:4966–4971.

33. Ochoa-Espinosa, A., G. Yucel, …, S. Small. 2005. The role of binding site cluster strength in Bicoid-dependent patterning in *Drosophila*. *Proc. Natl. Acad. Sci. USA.* 102:4960–4965.

34. Zinzen, R. P., K. Senger, …, D. Papatsenko. 2006. Computational models for neurogenic gene expression in the *Drosophila* embryo. *Curr. Biol.* 16:1358–1365.

35. Zeitlinger, J., R. P. Zinzen, …, M. Levine. 2007. Whole-genome ChIP-chip analysis of Dorsal, Twist, and Snail suggests integration of diverse patterning processes in the *Drosophila* embryo. *Genes Dev.* 21:385–390.